Print ISSN 2682-3993
Online ISSN 2682-4000

Assessment of the Efficiency and Economic Viability of an Upgraded Vacuum Membrane Distillation Setup for Ethanol-Water Separation

R.M.Zarraa[1,2], Shaaban Nosier[3], A.A. Zatout[3] ,Mohammed S.Al-Geundi[2]

1 Petrochemical Engineering Department, Faculty of Engineering, Pharos University in Alexandria, Alexandria, Egypt.

2 Chemical Engineering Department, Faculty of Engineering, Minia University, Minia, Egypt.

3 Chemical Engineering Department, Faculty of Engineering, Alexandria University, Alexandria, Egypt.

Abstract- Membrane distillation is a promising technique for extracting organic molecules from water mixtures. It works by applying pressure and heat differentials across hydrophobic microporous membranes. This work uses pre-prepared Polyvinylidene fluoride membranes to explore vacuum membrane distillation (VMD) at both laboratory and pilot scales. Ethanol-water solutions with different ethanol concentrations (2%, 5%, 7%, and 10%), temperatures (293 K to 333 K), and feed flow rates (0.06 to 0.18 L/s) are used to assess the system's performance. The separation factor ranges from 4 to 9.6, and at 328 K, 10 weight percent ethanol, and a feed flow rate of 0.18 L/min, a maximum total membrane flux of 44 kg/m²hr is attained. To ascertain whether VMD for ethanol-water separation is economically feasible, cost indicators are also evaluated. Based on a preliminary assessment using a 174 L/day pilot unit, it is possible that capital and operational costs will decrease as the technology develops and is scaled up, especially if low-grade energy sources are used.

Keywords- Membrane distillation, Polyvinylidene fluoride membranes, Ethanol-water solutions

I. INTRODUCTION

Regarding the expansion of the global population, numerous developing nations face challenges related to water scarcity due to limited resources and escalating freshwater demands [1]. To address this issue, effective water management initiatives are crucial in various regions worldwide. Water desalination emerges as a viable solution. Industrial-scale desalination technologies are typically categorized into two primary groups: thermal processes (such as Multi-Stage Flash distillation, Multi-Effect Distillation, and Vapor Compression) and membrane processes (including Reverse Osmosis and Electro Dialysis Reversal). Despite their commercialization, these technologies often entail significant energy consumption, encounter scalability issues, and face operational challenges.

An alternative approach, Membrane Distillation (MD), is considered a promising technology due to its potential advantages in energy efficiency, simplicity, and compatibility with solar energy [2,3]. MD represents a novel method in desalination and water treatment. It operates based on temperature and pressure differentials, enabling water to evaporate through a hydrophobic microporous membrane. This process ensures high water purity regardless of the feedwater quality, with the vapor subsequently condensing into a freshwater stream [1,4,5]. The driving force for mass transfer in MD is the vapor pressure difference created by a temperature gradient across the membrane. Because the partial vapor pressure of water is minimally affected by higher concentrations of dissolved salts, MD holds promise as an effective method for treating highly saline feeds.

It also experiences significantly less membrane fouling than microfiltration, ultrafiltration, and reverse osmosis, and requires a smaller vapor space than traditional distillation. Additionally, membrane distillation effectively rejects dissolved, non-volatile species, operates at lower temperatures than traditional evaporation, and operates at lower pressures than pressure-driven membrane processes [6-10].

Various other methods are available for component separation. For instance, Air-assisted liquid–liquid microextraction is effective for extracting various analytes, including organic substances and medical analytes [11]. Liquid-liquid microextraction strategies based on the in-situ formation or decomposition of deep eutectic solvents have also been explored [12]. Additionally, air agitation has been utilized as a green co-factor with dispersive liquid–liquid microextraction solidified floating organic drop, addressing previous technique drawbacks [13].

Print ISSN 2682-3993
Online ISSN 2682-4000

Electrothermal atomic absorption spectrometry (ETAAS) is another method, particularly suitable for water treatment applications [14].
This study aims to propose a more efficient and cost-effective method for ethanol separation, which is crucial in industries such as biofuel production and pharmaceuticals. The findings from this research endeavor can significantly contribute to the advancement of sustainable and environmentally friendly separation processes.

II. MATERIALS AND METHODS

In this study, a vacuum membrane distillation cell (VMDC) was utilized, as shown in Figure 1. The cell consists of two separate compartments crafted from acrylic polymeric material to prevent corrosion and dissolution caused by the ethanol solution. The outer surface area of the cell measures 54 m2, with a polymeric PVDF membrane of 16 cm2 situated between the two polymeric compartments, acting as a separator. The lower section of the cell is divided into two parts: one for introducing the feed solution and the other for collecting the retentate, which is then recycled back to the feeding tank. The distance between these sections is approximately 2 cm. A vacuum is applied to the upper section of the cell (the permeate part) using a vacuum pump. The permeate is obtained by condensing the vapor flux exiting the upper section of the cell through the use of cold water circulated via the condenser. The condensed vapor, referred to as permeate, is then accumulated in a permeate tank.

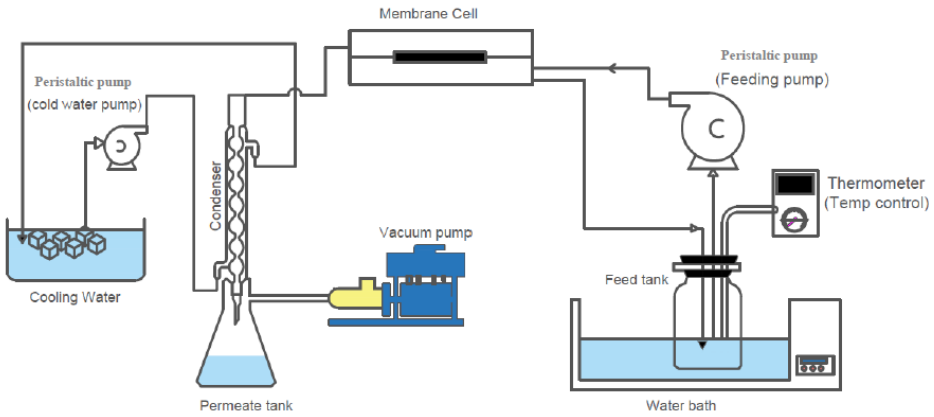

Fig 1. Schematic Representation of the Laboratory-Scale Vacuum Membrane Distillation Apparatus

Various concentrations of the ethanol-water mixture were prepared for the synthetic feed solution, including 2, 5, 7, and 10 wt.%. The temperature of the feed solution ranged from 20 to 60 ℃, and flow rates varied from 0.064 to 0.179 L/min, regulated by a peristaltic pump. To evaluate the ethanol passing through the membrane, the ethanol content in the collected aqueous solution from the permeate tank was determined.

Before each experimental run, 2 liters of the synthetic feed solution were placed in the feed tank and allowed to circulate through the cell membrane for one hour. During this time, no sample was taken from the permeate tank for ethanol concentration analysis. The separation factor was then calculated based on the measured concentration using equation (1).

$$\alpha_{Eth-H_2O} = \frac{\left(x_{Eth,P}/x_{w,P}\right)}{\left(x_{Eth,F}/x_{w,F}\right)} \qquad (1)$$

The total permeates flux and ethanol permeate flux was determined by the following equations (2) and (3)

$$J_{tot} = \frac{w_p}{A \times t} \qquad (2)$$

$$\mathrm{J_{Eth,t}} = \frac{\mathrm{w_{Eth,p}}}{\mathrm{A \times t}} \qquad (3)$$

Print ISSN 2682-3993
Online ISSN 2682-4000

III. RESULTS AND DISCUSSION

Figure (2) demonstrates how the total permeate flux changes with different volumetric flow rates, alongside with varying initial ethanol concentrations in the feed. It's noticeable that higher feed flow rates correspond to an increase in total permeate flux. This can be attributed to two factors:

Two resistance mechanisms occur during membrane separation: a. Hindrance to mass transfer due to the thickness of the concentration boundary layer on the membrane feed side. b. Resistance from the membrane itself, which is linked to the first resistance. As the feed rate rises, the concentration boundary layer becomes thinner, resulting in an improvement in the mass transfer coefficient and the mass transfer rate.

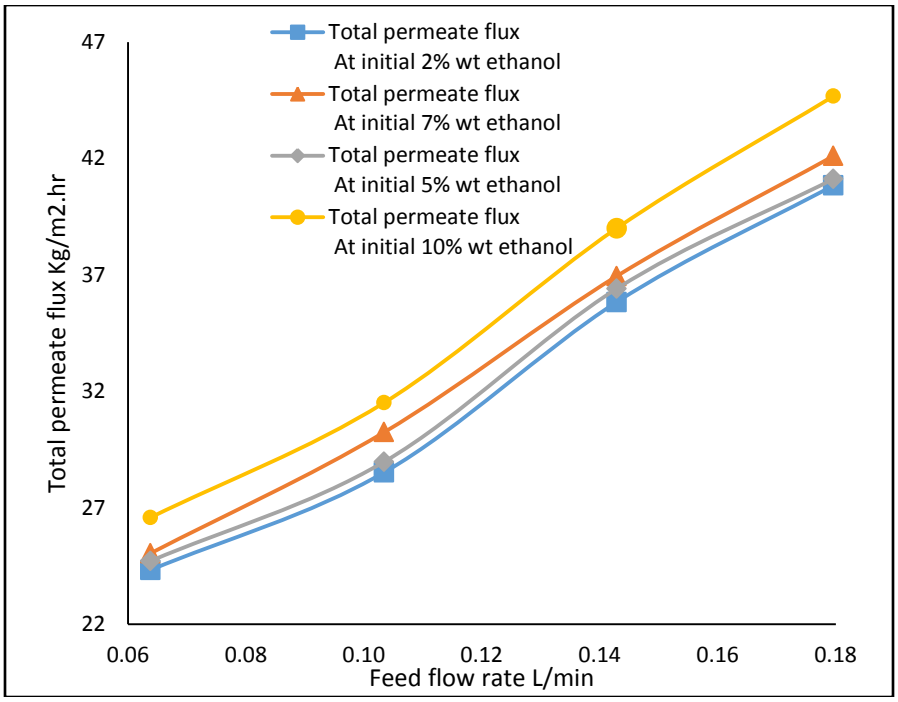

Fig 2.the outcome of volumetric flow rate on the total permeate flux at different initial ethanol concentration in the feed

However, the resistance to mass transfer at the membrane's inlet remains constant regardless of the flow rate and is primarily determined by the membrane's properties such as porosity, mean pore size, and thickness. Increased ethanol transport through the membrane can be facilitated by higher membrane porosity, larger average pore size, and thinner membrane thickness. Moreover, lower flow rates may result in water's convective mass transfer resistance becoming dominant, leading to an increase in membrane flux with higher feed rates. However, a higher feed flow rate may introduce more mass transfer resistance across the membrane, potentially hindering an increase in flux despite the rise in feed velocity.

At 50 °C, increasing the feed flow rate from 0.064 L/min to 0.103 L/min resulted in a 68% increase in permeate flux compared to that at a flow rate of 0.064 L/min across different initial ethanol side due to turbulence, consequently augmenting permeate flux.

Additionally, at the same temperature of 50 °C, Figure (3) illustrates the impact of the feed flow rate on the total ethanol concentration at different initial ethanol concentrations. This can be attributed to the following factors:

The hydrophobic nature of the membrane, which makes it highly selective towards ethanol over water.

At higher feed concentrations, water exhibits lower volatility compared to ethanol, resulting in reduced vapor production. This enhances ethanol flow across the membrane and exerts a significant partial vapor pressure on the membrane side of the feed.

Print ISSN 2682-3993
Online ISSN 2682-4000

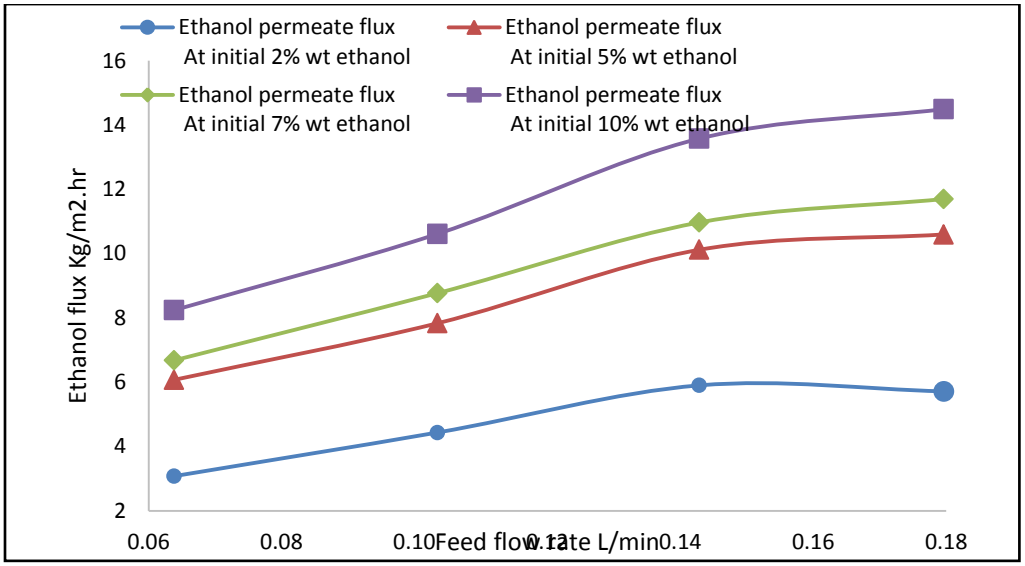

Fig 3.the effect of feed flow rate on the total ethanol concentration and at a temperature of 50 °C

At a temperature of 50°C and with varying initial ethanol concentrations, Figure (4) demonstrates the effect of feed flow rate on the separation factor at different initial ethanol concentrations. The separation factor increases as the feed flow rate rises from 0.064 L/min to 0.143 L/min, but subsequently decreases with a further increase in the feed flow rate to 0.179 L/min.

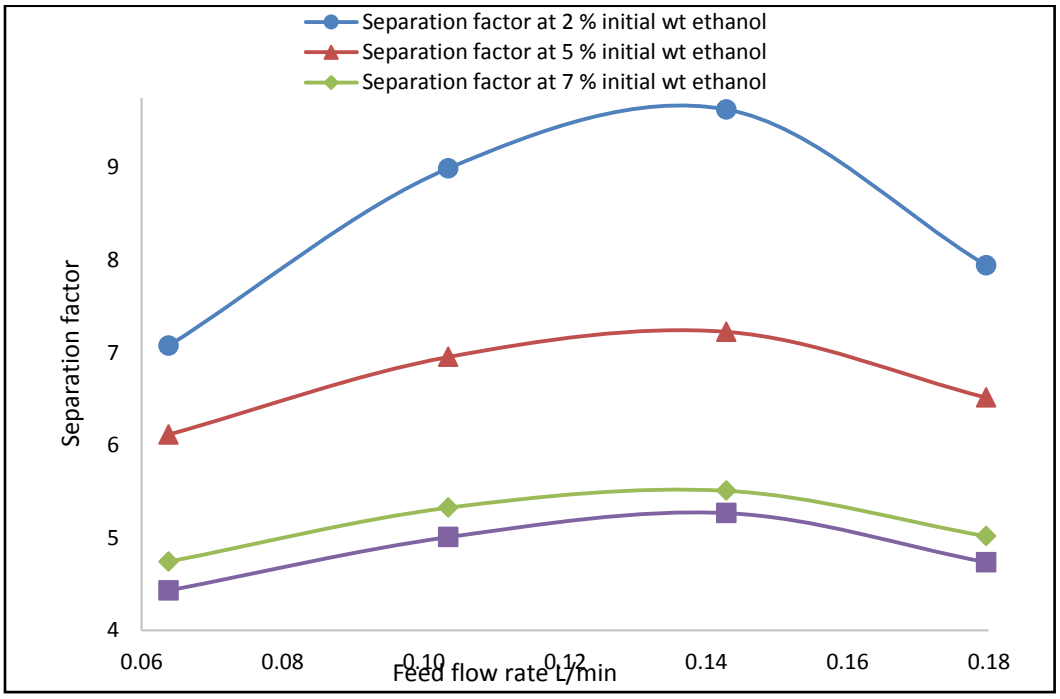

Fig 4.the effect of feed flow rate on the separation factor at a temperature of 50 °C and different initial concentration of ethanol

Print ISSN 2682-3993
Online ISSN 2682-4000

At a specific feed flow rate, there's a decrease in the separation factor as the initial ethanol concentration rises. This decline may be due to the increased ethanol concentration leading to higher solution viscosity, which subsequently reduces the mass transfer rates of both total and ethanol permeate, resulting in a lower separation factor. Figures 5 and 6 shows the effect of changing initial ethanol concentrations on the Ethanol flux and separation factor at different feed flow rates.

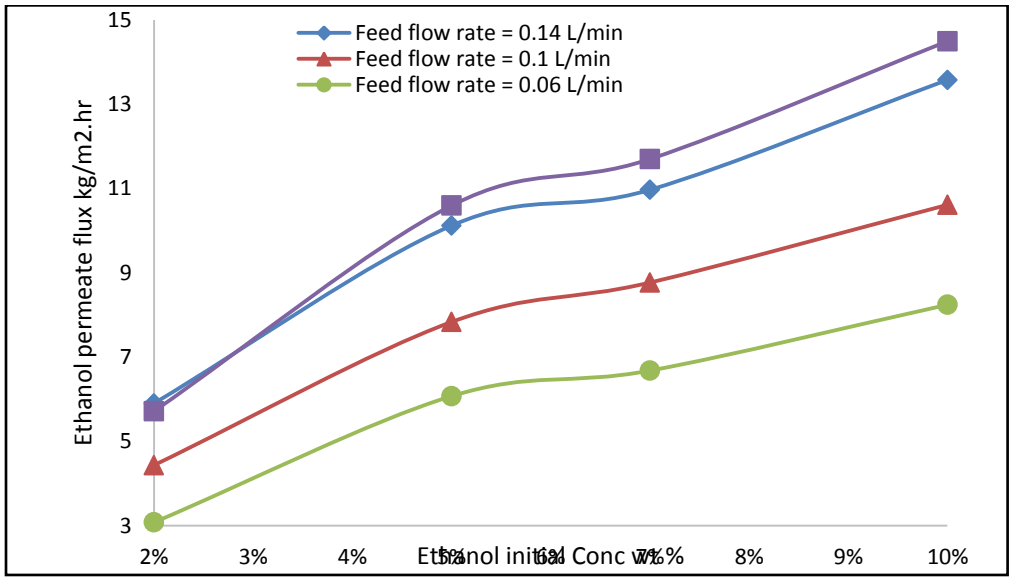

Fig 5. the impact of the ethanol's starting concentration on the ethanol permeate flux at various feed flow rates at a 50 °C

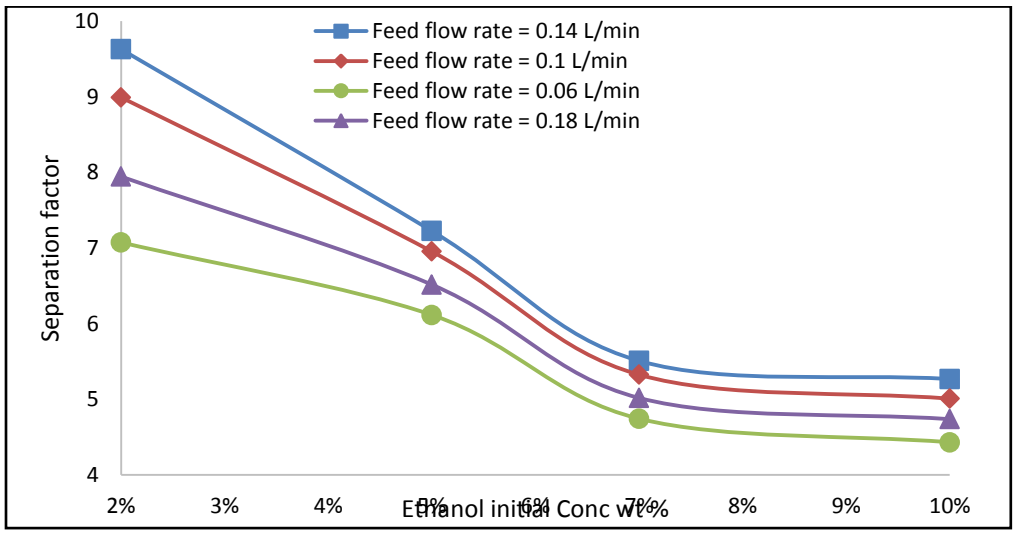

Fig 6. the impact of the initial ethanol content on the separation factor at various input flow rates at 50 °C

Temperature's influence was studied by adjusting the feed temperature from 20°C to 60°C [36], in increments of 10°C Over one hour, while maintaining a feed flow rate of 0.0103 m^3/min and an initial ethanol concentration of 2 wt%.[15]

Figures 7, 8, and 9 display that as the feed temperature increases, both the total permeate flux and ethanol permeate flux, along with the separation factor, also increase.

Print ISSN 2682-3993
Online ISSN 2682-4000

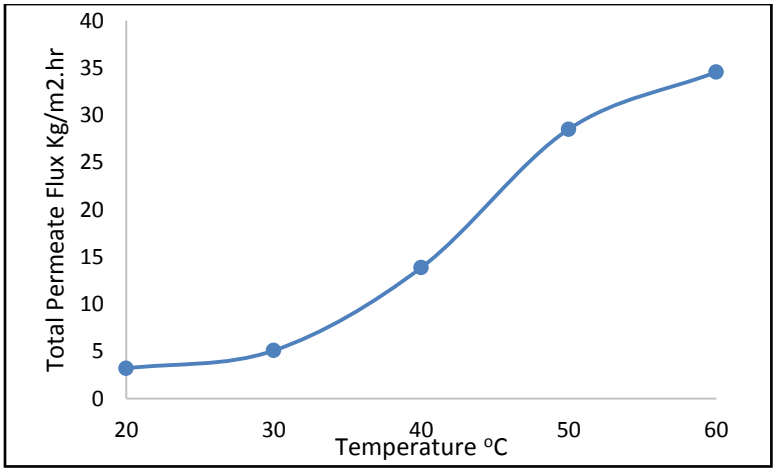

Fig 7. The temperature's impact on total permeate flux at 0.1 L/min feed rate and 2% starting ethanol concentration

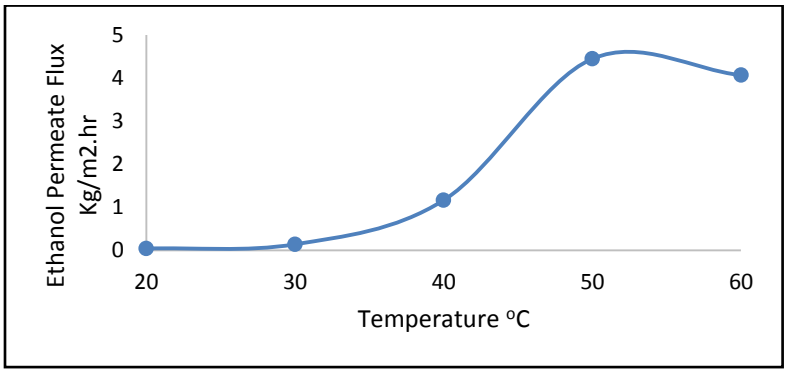

Fig 8. The impact of temperature on the ethanol permeate flux at 0.1 L/min and 2% wt starting ethanol concentration.

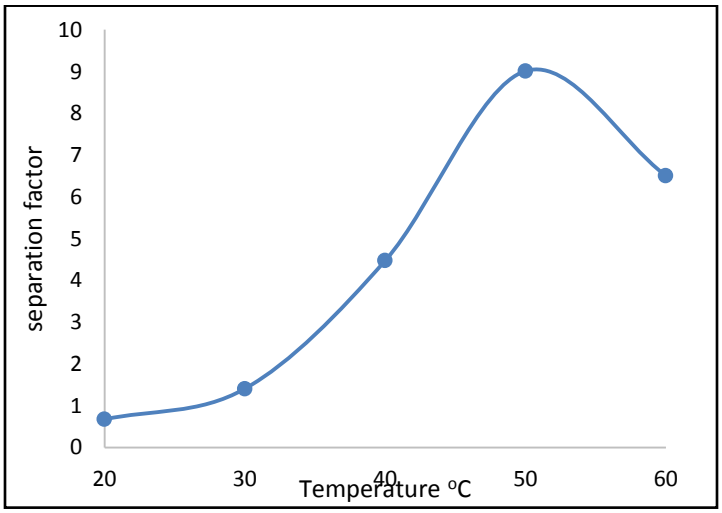

Fig 9. The impact of temperature on the separation factor at 0.1 L/min and 2% wt starting ethanol concentration.

This could occur due to the increased vapor pressure of ethanol and water. However, above 50°C, there was a sudden decrease in both ethanol flux and separation factor. This might be attributed to the conflicting influences of molecule size and boiling point of the components. Despite being smaller, ethanol molecules have a lower boiling

Print ISSN 2682-3993
Online ISSN 2682-4000

point compared to water molecules. Consequently, there could be a competition between vapor generation and molecular diffusion rates across the membrane.

IV. ECONOMIC EVALUATION

- Preliminary Economic Evaluation

Assessment of the vacuum membrane distillation process, as a new technology for separation of ethanol from water ethanol mixture, a preliminary evaluation is performed based on the information acquired for implementing a pilot unit of 174 L/day from the local marketing.

- Lab scale instruments used

Table 1 shows the instruments that were used in performing this experiment at lab scale

Table 1 Instruments used in lab scale experiment

Item	Description
1	2 storage tanks, 3L
2	Vacuum pump 0.5 Horse power
3	Feeding pump 0.25 Horse power
4	Water pump 0.1 Horse power
5	Condenser and water pump
6	Connections
7	Heater 0.8 Horse power
8	Membrane distillation module

- Process Design

Based on the results of the performance of the VMD pilot system operating with an average total permeate flux of 55.53 kg/m2h (58.88 L/ m2h); the basic design of a pilot plant unit is developed as follows:
Design capacity: 174 L d-1
Area of one membrane sheet: 0.011 m2
Total mass transfer area: 0.1168 m2
Feed flow rate: 14.6 L/h
Average Ethanol feed concentration: 2% wt
Module: plate and frame module of 10 sheets.
Feed temperature: 50 ℃
Vacuum pressure: 0.01 kPa
Table 2 shows equipment used in pilot plant scale membrane distillation.

Table 2 Equipment used in pilot plant scale

Item	Features and operating conditions
Feed Tank	Fiberglass feed tank, volume: 3.7 m3, 1.5 m diameter, 2 m height.
Membrane distillation module	PVDF hydrophobic porous membrane, of square cross section of 0.1*0.1 m2
Ethanol water mixture stream	The ethanol water mixture stream is recycled to the feed tank
Product tank	Fiberglass product tank, volume: 0.1767 m3, 0.5 m diameter, 0.9 m height.
Heat Exchanger (Condenser)	Stainless steel 316 L condenser with heat transfer area of 0.1 m2, hot fluid: produced water vapor (Tv = 50 ℃), cold fluid: feed water (Tf = 20 ℃)
Feeding Pump	Feed pump: centrifugal pump of stainless steel 316L, with rate of discharge range from 40 cm3s-1 of 0.25 Hp. motor drive
Vacuum pump	Double stage vacuum pump, 5×10-1Pa /3.75 Micron, 0.75 Hp

Print ISSN 2682-3993
Online ISSN 2682-4000

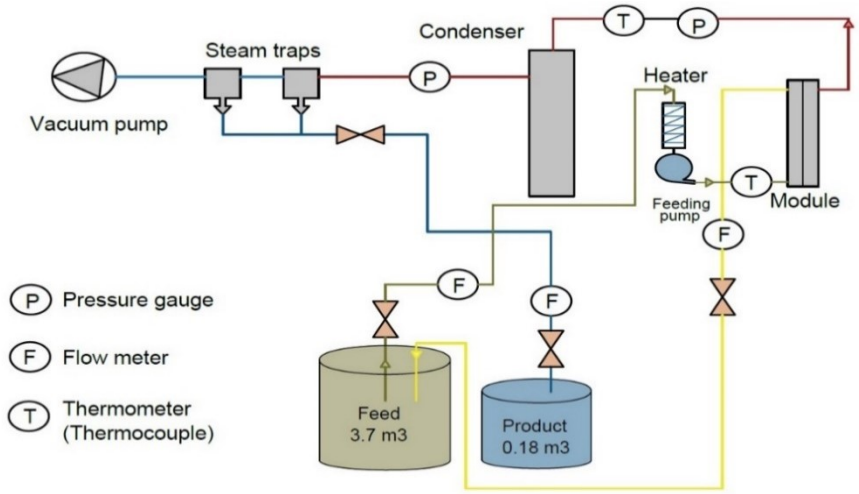

Fig 10. Schematic diagram for pilot test vacuum membrane distillation

- Product Cost Estimation

Table 3 depicts the price list for purchasing and implementing the prototype unit. This price offers the total fixed capital investment of the unit [16].

Table 3 Total fixed capital investment of the pilot plant unit.

Item	Description	Price ،LE	Life time
1	Membrane holder for 10 membrane sheets, 0.1*0.1 m2	260000	3 years
2	Unit base		
3	Heater		
4	Temperature degree measuring device		
5	Control panel		
6	Pressure gauge		
7	Steam traps		
8	Condensation system	12000	
9	Vacuum pump	20000	
10	Feeding pump, 0.25 Hp	22000	
11	Two tanks	7000	
Equipment cost		321000	
Piping and Instrumentation (30% of Equipment Cost)		96300	
Total fixed capital investment		417300	

Total Fixed capital investment is the sum of the equipment cots including their installation and also the piping and instrumentation cost which is assumed to be 30 % of the equipment cost according to what mentioned in references [16]

Depreciation was calculated using straight line method and assuming salvage value of all equipment after the project life time which is assumed to be 3 years is zero

$$\text{Depreciation} = \frac{equipment\ cost - salvage\ value}{project\ life\ time} \quad (4)$$

Where all other assumptions mentioned in Table 4 where assumed from literature [16]

Accordingly, the annual operating costs- including the depreciation- are depicted in Table 4

Print ISSN 2682-3993
Online ISSN 2682-4000

Table **Error! No text of specified style in document.** Annual operating costs- including the depreciation

Items	Cost LE/year
Depreciation	139100
Raw materials cost	575532
Membrane cost	1918
Labor assumption cost (2 workers)	48000
Energy cost	12,200.00
Maintenance (2% of depreciation)	2782
Overhead (50 % of labor cost)	24000
Total operating cost	803532
Contingency (2% of Total Operating Cost)	16070.64
Total produced Ethanol cost LE/L	14.33

The unit production cost of ethanol, produced by the VMD system with 90% plant availability, can be calculated as shown in table 4 [17,18]
The Cost of production of 1 L of ethanol = (total operating cost + contingency) / yearly production rate of ethanol at 90% plant availability = 14.33 LE/L

V. CONCLUSION

The study has successfully demonstrated several key findings:

1. The efficacy of vacuum membrane distillation (VMD) employing both a commercial polyvinylidene difluoride (PVDF) membrane for ethanol separation from a synthetic ethanol-water mixture.
2. The pivotal role of feed temperature in influencing permeation flux, as evidenced by experimental observations.
3. An increase in the initial ethanol concentration of the water-ethanol mixture resulted in a reduction in separation factor but an increase in both total permeate flux and ethanol flux. Moreover, augmentation of feed flow rate correlated positively with total permeate flux, ethanol flux, and separation factor.
4. A notable decline in ethanol flux and separation factor was observed at temperatures exceeding 50 °C, attributable to the interplay of molecule size and component boiling point.
5. These findings underscore the potential for achieving greater ethanol yields through the application of modified membranes.
6. The results contribute to the advancement of sustainable and efficient techniques for volatile component separation and offer valuable insights for refining the VMD process.
7. An Economic analysis revealed a competitive ethanol production cost of 14.33 LE/L, suggesting profitability in the local market context.

Print ISSN 2682-3993

Online ISSN 2682-4000

REFERENCES

[1] A. Alkhudhiri, N. Darwish, N. Hilal, Membrane distillation: A comprehensive review. Desalination., **287**, 2–18, 2012.

[2] M. Gryta, Effectiveness of water desalination by membrane distillation process, Membranes Journal., **2(3)**, 415-429, 2012. [3] A. Kullab, A. Martin, Membrane distillation and applications for water purification in thermal cogeneration plants,
Separation and Purification Technology., **76**, 231–237, 2011.

[4] B. Li, K. K. Sirkar, Novel membrane and device for vacuum membrane distillation-based desalination process, Journal of Membrane Science., **257**, 60–75, 2005.

[5] C. R. Martinetti, A. E. Childress, T. Y. Cath, High recovery of concentrated RO brines using forward osmosis and membrane distillation, Journal of Membrane Science., **331**, 31–39, 2009.

[6] L. Bazinet, C. Cossec, H. Gaudreau, Y. Desjardins, Production of a Phenolic Antioxidant Enriched Cranberry Juice by Electrodialysis with Filtration Membrane, J. Agric. Food Chem. 57 (2009) 10245–10251. https://doi.org/10.1021/JF9021114.

[7] D.S. Couto, M. Dornier, D. Pallet, M. Reynes, D. Dijoux, S.P. Freitas, L.M.C. Cabral, Evaluation of nanofi ltration membranes for the retention of anthocyanins of açai (euterpe oleracea mart.) juice, Desalin. Water Treat. 27 (2011) 108–113. https://doi.org/10.5004/DWT.2011.2067.

[8] F. dos Santos Gomes, P. Albuquerque da Costa, M.B. Domingues de Campos, S. Couri, L.M.C. Cabral, Concentration of watermelon juice by reverse osmosis process, Desalin. Water Treat. 27 (2011) 120–122. https://doi.org/10.5004/DWT.2011.2073.

[9] A.L. Quoc, M. Mondor, F. Lamarche, J. Makhlouf, Optimization of electrodialysis with bipolar membranes applied to cloudy apple juice: Minimization of malic acid and sugar losses, Innov. Food Sci. Emerg. Technol. 12 (2011) 45–49. https://doi.org/10.1016/J.IFSET.2010.12.007.

[10] I. Santana, P.D. Gurak, V.M. da Matta, S.P. Freitas, L.M.C. Cabral, Concentration of grape juice (vitis labrusca) by reverse osmosis process, Desalin. Water Treat. 27 (2011) 103–107. https://doi.org/10.5004/DWT.2011.2066.

[11] E.A. Azooz, H.S.A. Al-Wani, M.S. Gburi, E.H.B. Al-Muhanna, Recent modified air-assisted liquid-liquid microextraction applications for medicines and organic compounds in various samples: A review, Open Chem. 20 (2022) 525–540. https://doi.org/10.1515/CHEM-2022-0174/ASSET/GRAPHIC/J_CHEM-2022-0174_FIG_004.JPG.

[12] R. Ahmadi, E.A. Azooz, Y. Yamini, A.M. Ramezani, Liquid-liquid microextraction techniques based on in-situ formation/decomposition of deep eutectic solvents, TrAC Trends Anal. Chem. 161 (2023) 117019. https://doi.org/10.1016/J.TRAC.2023.117019.

[13] E.A. Azooz, M. Tuzen, W.I. Mortada, Green microextraction approach focuses on air-assisted dispersive liquid–liquid with solidified floating organic drop for preconcentration and determination of toxic metals in water and wastewater samples, Chem. Pap. 77 (2023) 3427–3438. https://doi.org/10.1007/S11696-023-02714-6/METRICS.

[14] D.J. Butcher, Recent advances in graphite furnace atomic absorption spectrometry: a review of fundamentals and applications, Https://Doi.Org/10.1080/05704928.2023.2192268. (2023). https://doi.org/10.1080/05704928.2023.2192268.

[15] E.A. Azooz, A greenness evaluation and environmental aspects of solidified floating organic drop microextraction for metals: A review, Trends Environ. Anal. Chem. 37 (2023) e00194. https://doi.org/10.1016/J.TEAC.2022.E00194

[16] M.S. Peters, K.D. Timmerhaus, Plant design and economics for chemical engineers /, McGraw-Hill, 1991. https://www.dioneoil.com/uploads/6/8/7/4/6874938/plant_design_and_economics_for_chemical_engineers.pdf (accessed February 4, 2024).

[17] S. Al-Obaidani, E. Curcio, F. Macedonio, G. Di Profio, H. Al-Hinai, E. Drioli, Potential of membrane distillation in seawater desalination: Thermal efficiency, sensitivity study and cost estimation, J. Memb. Sci. 323 (2008) 85–98. https://doi.org/10.1016/J.MEMSCI.2008.06.006.

[18] L.M. Camacho, L. Dumée, J. Zhang, J. de Li, M. Duke, J. Gomez, S. Gray, Advances in membrane distillation for water desalination and purification applications, Water (Switzerland). 5 (2013) 94–196. https://doi.org/10.3390/W5